Desalination and Water Treatment
www.deswater.com
doi: 10.1080/19443994.2014.939514

55 (2015) 3330–3335
September

Taylor & Francis
Taylor & Francis Group

Characterization of the microscopic mechanics in falling film evaporation outside a horizontal tube

Luopeng Yang*, Zhexuan Xu, Xiaohong Zhang, Shengqiang Shen

School of Energy and Power Engineering, Dalian University of Technology, Dalian 116024, China, Tel. +86 13130403891; Fax: +86 411 84707963; email: yanglp@dlut.edu.cn

Received 30 March 2014; Accepted 12 June 2014

ABSTRACT

In order to get a deep insight of the heat transfer mechanism of falling film evaporation outside a horizontal tube, the characterization of the microscopic mechanics was numerically investigated. A numerical model was developed to obtain the dynamic and heat transfer performance including film thickness, film velocity, film temperature and local heat transfer coefficient. The simulated results were found to be in a good agreement with the reported data. The results show that the convection plays an important role in the thin film evaporation even at low Reynolds number through the analysis on the profiles of the local film velocity and local heat transfer coefficient in the falling film. The distribution of the thermal developing region and thermal developed region along the tube circumference for a single tube and a tube bundle was predicted. The local film temperature increases and local heat transfer coefficient stabilizes at the top thermally developing region while the former stabilizes and the latter decreases at the fully thermal developed region which is at the bottom part of the tube.

Keywords: Characterization of the microscopic mechanics; Falling film evaporation outside a horizontal tube; Convection; Thermal developing region; Thermal developed region

1. Introduction

The horizontal-tube falling film evaporator occurs in numerous energy conversion and transport applications, including seawater desalination, refrigeration and air conditioning systems, chemical reactors and process industry heat exchange equipment. This type of evaporator provides a very effective means of transporting energy due to its advantages over other evaporators as small temperature difference, external thin film thickness and phase change on both sides of a tube. Detailed understanding of the heat transfer mechanism of falling film evaporation outside a horizontal tube is required to develop a sound designing method.

Although falling film evaporation is widely used, the information in the literature for its heat transfer mechanism is still limited. Most attention of prior experiments was directed towards how the experimental parameters affect the heat transfer performance. The heat flux was found to have no effect on

*Corresponding author.

Presented at the Conference on Desalination for the Environment: Clean Water and Energy 11–15 May 2014, Limassol, Cyprus

heat transfer coefficients for convection conditions [1–4] while the heat transfer coefficients were reported to increase with the heat flux for boiling evaporation [5–7]. This can be explained by their heat transfer mechanisms of film evaporation and nuclear boiling evaporation, respectively.

Many researchers have experimentally shown diverged behaviours of the liquid film flow rate effect in convection conditions: as the flow rate increases, the heat transfer coefficient increases after it decreases to a minimum [8,9], the heat transfer coefficient is independent on the flow rate [7,10] and the heat transfer coefficient increases [1,11]. This could possibly attribute to the change of the falling film flow models which correspond to different liquid film profiles.

Numerous comprehensive experiments [1,4,12] confirmed that the heat transfer coefficient increases with liquid film temperature. This temperature effect is due to the decrease in liquid viscosity which consequently thins the liquid film.

A great deal of experimental efforts have been limited on the measurement of heat transfer coefficients for falling film evaporation outside a horizontal tube. These measurements are useful in providing boundary conditions and qualitative information, but they can not give a real insight as to the true nature of liquid and vapour flows and their interactions. There appears to be few experimental data on the microscopic mechanics of liquid film which includes local film thickness, velocity and temperature profile in the falling film due to the challenge inherent in the measurement.

Empirical correlations for the horizontal-tube falling film evaporation are intended to generate heat transfer coefficient, pressure drop and wall shear using liquid flow rate, entrance temperature and pressure as their inputs. A great number of correlations [1,3,13–16], which are selected in terms of an assessment of the flow regime, the falling film flow mode and the prevailing heat transfer mechanism, are widely proposed. However, due to the complexity of the two-phase flow, the designation of the flow regimes and flow modes has not yet been standardized and generally depends on the researchers' arbitrary judgement. The development of the correlations is limited to relatively few flow conditions and test sections.

A significant amount of simulation work has been performed. The flow and heat transfer of the falling film evaporation along a horizontal tube is classified into different regions where analytical models are proposed [8,13,17]. But their calculations do not agree with each other on the distribution of the fully developed region. A range of simulation models [18–21] have been proposed to describe the local heat transfer performance based on assumptions of the temperature and velocity profiles in the film. However, the hypothesized profiles appear to lead to diverged outcomes.

In light of the previous literature review, although the mathematical and experimental research that is mainly on heat transfer performance, exists for falling film evaporation outside a horizontal tube, very few attempt to determine the profiles of the temperature and velocity in the film in order to explore the microscopic mechanics. Since the heat transfer performance is closely tied to the distribution of the film velocity and temperature and most theoretical models are based on the hypothesized distribution, it is significant that the profiles of the temperature and velocity be determined as part of the model solution.

In order to get a deep insight of the heat transfer mechanism of falling film evaporation outside a horizontal tube, the characterization of the microscopic mechanics was numerically investigated. The dynamic and heat transfer performance, including film thickness, film velocity, film temperature and local heat transfer coefficient, was simulated. The detailed information was described to understand the fundamental mechanics of momentum and energy transport in two-phase falling film flow.

2. Mathematical models

A schematic of falling-film evaporation outside a horizontal tube is demonstrated in Fig. 1. Falling liquid with the mass flow density of 2Γ impinges on the top of the horizontal tube and wets both sides of the tube. The liquid film flows along the circumference and drains down to the bottom of the tube.

The N–S equations can be simplified by the following assumptions:

(1) The properties of liquid are uniform in per unit length of the tube at the temperature of $\frac{(T_W+T_V)}{2}$. And the ambient pressure is constant and corresponds to the saturated temperature.

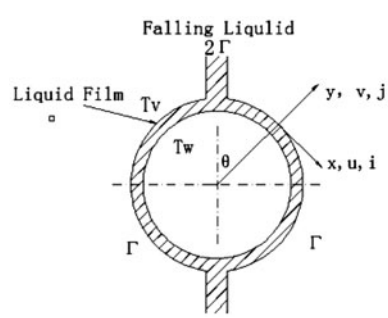

Fig. 1. Schematic of falling-film evaporation outside a horizontal tube.

(2) There are no considerations about the shear stress and pressure gradient on the circumferential film outside the tube.
(3) Due to the thin film compared with the tube diameter, the influence of the curve is neglected.
(4) The liquid free falling on the top of the tube is the same as a jet impinging on a flat surface.

The continuity, momentum and energy equations are as follows:

$$\frac{\partial u}{\partial x}+\frac{\partial v}{\partial y}=0 \tag{1}$$

$$u\frac{\partial u}{\partial x}+v\frac{\partial v}{\partial y}=g\sin(x/R)+\upsilon\frac{\partial^2 u}{\partial y^2} \tag{2}$$

$$u\frac{\partial T}{\partial x}+v\frac{\partial T}{\partial y}=\frac{k}{\rho C_p}\frac{\partial^2 T}{\partial y^2} \tag{3}$$

The low density is expressed as:

$$\Gamma=\rho\int_0^\delta u dy \tag{4}$$

The starting velocity near the impinging point on the tube top is given as [22]:

$$u_0=C_x[(2\eta-3\eta^3+\eta^4)+\frac{\Lambda}{6}(\eta-3\eta^2+3\eta^3-\eta^4)] \tag{5}$$

$$v_0=0$$

where $\eta=y/\sigma_b$

$$\sigma_b=(\Lambda v_f/C)^{0.5}$$

$$\Lambda=\left(\frac{\sigma_b}{v_f}\frac{du}{dx}\right)$$

The boundary conditions are listed as:

$$\begin{array}{l} \text{at } y=0,\quad x>0\ u=0,\quad v=0 \\ \text{at } y=\delta,\quad x>0,\quad \frac{\partial u}{\partial y}=0 \end{array} \tag{6}$$

at $y>0$, $x=0$, $u=u_0$, $v=v_0$
at $y=0, x>0\ -\left(k\frac{\partial T}{\partial y}\right)_{y=0}=q$ constant flux.
$T=T_w$ constant wall temperature
at $y=\delta, x>0\quad T=T_V$.

Local heat transfer coefficient can be obtained as:

$$\mathrm{h}(\theta)=\frac{q}{T_W-T_V}=\frac{\left(k\frac{\partial T}{\partial y}\right)_{y=0}}{T_W-T_V} \tag{7}$$

The transition inclination angle is determined according the recommendation of Chyu and Bergles [8]:

$$\Phi=\frac{1}{\pi\alpha R}\left(\frac{3\mu\Gamma^4}{g\rho^5}\right)^{1/3} \tag{8}$$

3. Results and discussion

The numerical results of local and average heat transfer coefficient and film thickness over a horizontal tube with a constant heat flux are compared with the measured data of Liu [10] and Solan or Zfato [23] in Fig. 2.

The calculated prediction shows a good agreement with the experimental results. The proposed model for falling film evaporation is proved to be reliable to predict the heat transfer characteristics. The calculated local heat transfer coefficients, shown in Fig. 2(c), are overestimated near the upper apex and underestimated near the bottom of the tube. As both regions accounts for a very small part of the circumferential length of the tube, this discrepancy has little effect on the average heat transfer coefficients.

Fig. 3 presents the radial velocity profile in the liquid film, including the interface velocity of $V_{\text{interface}}$, the interior velocity of V_{interior} corresponding to the one of the third node away from the tube wall and averaged velocity of $V_{\text{average.}}$ When the inclination angle of ranges from 10˚ to 100˚, $V_{\text{interface,}}$ flowing towards the tube wall, is negative while V_{interior}, flowing outward to the wall, is positive. As a result, the convective effect is strengthened. When >100˚, all the radial velocities become positive, thus the convective effect is weakened. This result is proven in Fig. 4 which compares the local heat transfer coefficients between the numerical prediction and the Nusselt type solution along the circumference. Compared with the Nusselt's result, the predicted one is higher even at a small flow rate of Re = 200. The difference lies in the convective term in the energy equation and the inertia term in the momentum equation which is taken into account in the simulation model and is neglected in the Nusselt solution. It can also be seen that at θ about 17˚ where $V_{\text{interface}}$ is the lowest and the convective effect is the strongest, the divergence of local heat transfer coefficients is the biggest. When >100˚, the divergence is narrowed at a faster speed.

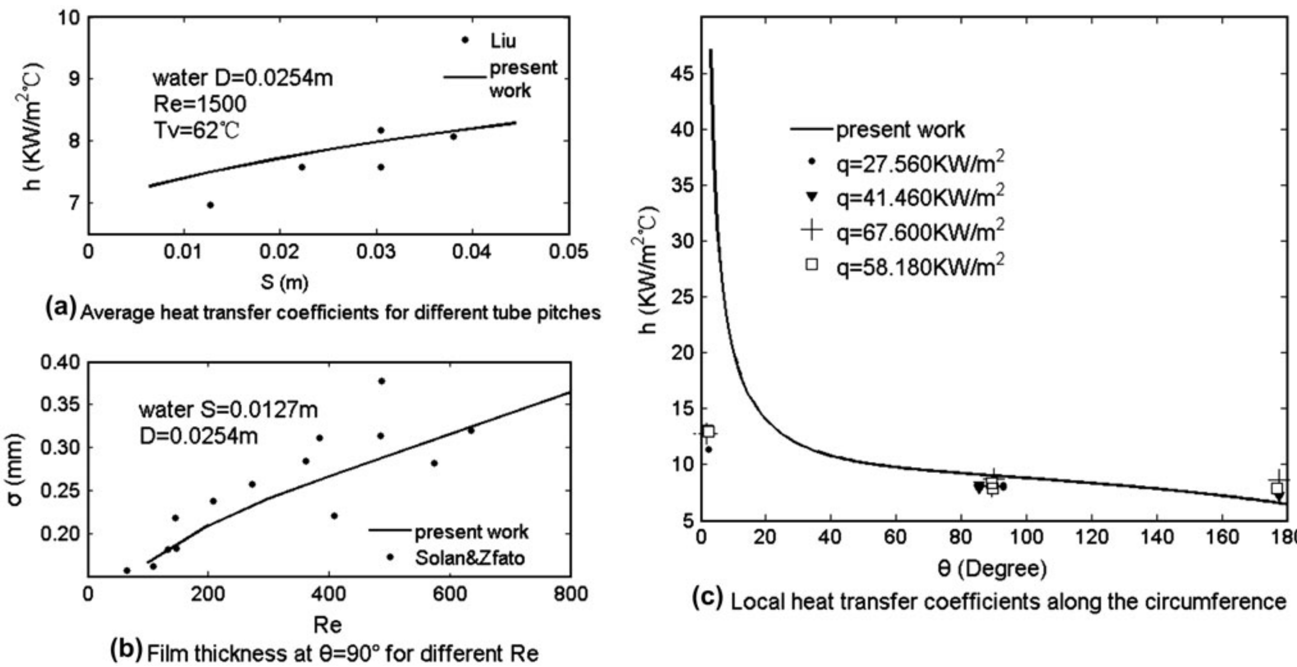

Fig. 2. Comparison of the present prediction with experimental data.

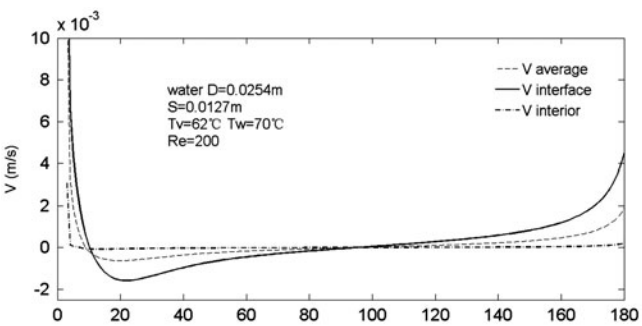

Fig. 3. Profile of radial velocity along the tube circumference.

Therefore, even for the flow of low Re that is considered to be laminar, the effect of the radial velocity on the convective heat transfer can not be neglected due to the very thin film on the outside of the tube at the magnitude of mm.

Fig. 5 shows a plot of local heat transfer coefficients, local film temperature as a function of inclination angle of and Re. For Re = 200 and Re = 400, the transition inclination angles between the thermally developed region and thermally developing region are 32.6° and 82.2°, respectively. For Re = 3,000, the whole tube circumference is covered by the thermally developed region. It is seen that the local film temperatures stay almost constant and the local heat transfer

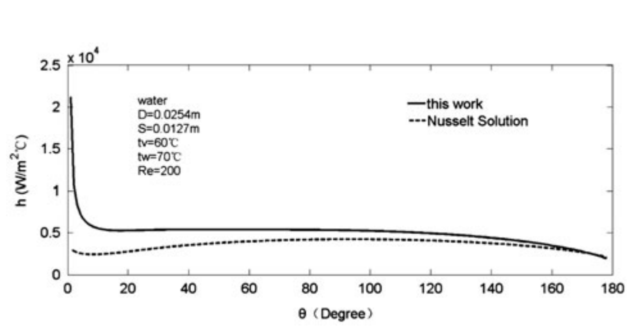

Fig. 4. Comparison of the local heat transfer coefficients for the prediction and the Nusselt solution.

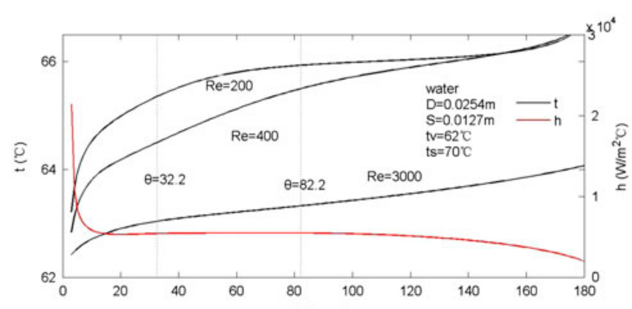

Fig. 5. Profile of local film temperature and local heat transfer coefficient.

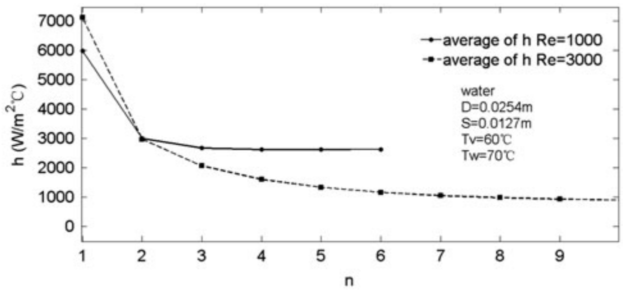

Fig. 6. Profile of average of heat transfer coefficients with tube number in a horizontal tube bundle.

coefficients reduce along the tube circumference in the thermally developed region where the thermal boundary layer extends across the whole film, and that the local film temperatures increase and the local heat transfer coefficients stabilize in the thermally developing region where the thickness of the thermal boundary layer is less than the film thickness. This fact can be attributed to the profile of the thermal boundary layer thickness. The results also show that the thermally developed region is reached at a small inclination angle for a small Re and that the thermally developing region is extended with an increase in Re.

Figure 6 shows the profile of average heat transfer coefficients for a tube bundle. It can be inferred that the first six tubes for Re = 3,000 and the first three tubes for Re = 1,000 are covered by the thermally developing region as the external heat transfer coefficients successively decrease with an increasing number of tube row and that the thermally developed region, where the heat transfer coefficients keep almost constant, is approached when $n > 6$ for Re = 3,000 and $n > 3$ for Re = 1,000, respectively.

4. Conclusions

A numerical model, which took into account the essentials of the hydrodynamics and film evaporation, was presented to solve the dynamic and heat transfer performance including film thickness, film velocity, film temperature and local heat transfer coefficient.

Comparison of the simulated local and average heat transfer coefficient and film thickness indicated a good agreement with the experimental data, which proves that the proposed model is reliable.

The profile of the radial velocity and the local heat transfer coefficient shows the microscopic mechanics in the liquid film and the role of the convection in the thin film evaporation.

The distributions of the thermal developing region and thermal developed region for a single tube and a tube bundle were predicted by the analysis of the profile of film temperatures and average heat transfer coefficients.

Nomenclature

C_P	—	specific heat at constant pressure J/(kg K)
D	—	diameter of tube (m)
g	—	acceleration of gravity (N/m^2)
h	—	heat transfer coefficient W/(m^2 ℃)
k	—	thermal conductivity W/(m^2 ℃)
q	—	heat flux (W/m^2)
R	—	outer radius of tube (m)
Re	—	Reynolds number
T	—	temperature (K)
T_V	—	temperature of surrounding (K)
T_W	—	temperature of tube wall (K)
U	—	tangential velocity (m/s)
V	—	radial velocity (m/s)
x	—	tangential
y	—	radial
δ	—	film thickness (m)
α	—	thermal diffusivity (m^2/s)
ρ	—	density (kg/m^3)
Γ	—	mass density (m^3/s)
θ	—	inclination angle, measured from the top of horizontal tube degree
υ	—	kinematic viscosity (m^2/s)
Φ	—	angular position of thermal developed region degree

Acknowledgement

This work was supported by the National Natural Science Foundation of China [grant number 51176019].

References

[1] W.H. Parken, L.S. Fletcher, V. Sernas, J.C. Han, Heat transfer through falling film evaporation and boiling on horizontal tubes, J. Heat Transfer 112 (1990) 744–750.

[2] Y. Fujita, M. Tsutsui, Evaporation heat transfer of falling films on horizontal tube. Part 2: Experimental study, Heat Transfer Jpn. Res. 24 (1995) 17–31.

[3] X. Hu, A.M. Jacobi, The intertube falling film. Part 2. Mode effects on sensible heat transfer to a falling liquid film, J. Heat Transfer 118 (1996) 626–633.

[4] X. Li, M.R. Ge, S.C. Wang, Y.X. Wang, Heat-transfer film coefficients of falling film horizontal tube evaporators, Desalination 66(15) (2004) 223–230.

[5] L.S. Fletcher, V. Sernas, W.H. Parken, Evaporation heat transfer coefficients for thin seawater films on horizontal tubes, Ind. Eng. Chem. Process Des. Dev. 14 (1975) 411–416.

[6] S.A. Moeykens, M.B. Pate, Spray evaporation heat transfer of R-134a on plain tubes, ASHRAE Trans. 100 (2) (1994) 173–184.

[7] X. Zeng, M.-C. Chyu, Z.H. Ayub, Evaporation heat transfer performance of nozzle-sprayed ammonia on a horizontal tube, ASHRAE Trans. 101(1) (1995) 136–149.
[8] M.-C. Chyu, A.E. Bergles, An analytical and experimental study of falling-film evaporation on a horizontal tube, J. Heat Transfer 109 (1987) 983–990.
[9] Y. Fujita, M. Tsutsui, Experimental investigation of falling film evaporation on horizontal tubes, Heat Transfer Jpn. Res. 27 (1998) 609–618.
[10] P. Liu, The Evaporating Falling-film on Horizontal Tube, PhD Thesis, University of Wisconsin-Madison, Wisconsin, August 1975.
[11] J.V. Putilin, V.L. Podberezny, V.G. Rifert, Evaporation heat transfer in liquid films flowing down horizontal smooth and longitudinally profiled tubes, Desalination 105 (1996) 165–170.
[12] Luopeng Yang, Shengqiang Shen, Experimental study of falling film evaporation heat transfer outside horizontal tubes, Desalination 220 (2008) 654–660.
[13] Z.H. Liu, Q.Z. Zhu, Y.M. Chen, Evaporation heat transfer of falling water film on a horizontal tube bundle, Heat Transfer Asian Res. 31 (2002) 42–55.
[14] X. Zeng, M.-C. Chyu, Z.H. Ayub, Ammonia spray evaporation heat transfer performance of single low-fin and corrugated tubes, ASHRAE Trans. 104(1A) (1998) 185–196.
[15] X. Zeng, M.-C. Chyu, Z.H. Ayub, Performance of nozzle sprayed ammonia evaporator with square-pitch plain-tube bundle, ASHRAE Trans. 103(2) (1997) 68–81.
[16] X. Zeng, M.-C. Chyu, Z.H. Ayub, Experimental investigation on ammonia spray evaporators with triangular-pitch plain tube bundle. Part II: Evaporator performance, Int. J. Heat Mass Transfer 44 (2001) 2081–2092.
[17] G. Kocamustafaogullari, I.Y. Chen, Falling film heat transfer analysis on a bank of horizontal tube evaporator, AIChE J. 34 (1988) 1539–1549.
[18] T. Nosoko, A. Miyara, The evolution and subsequent dynamics of waves on a vertically falling liquid film, Phys. Fluids 16 (2004) 1118.
[19] C.D. Park, T. Nosoko, Three-dimensional wave dynamics on a falling film and associated mass transfer, AIChE J. 49 (2003) 2715.
[20] V.Y. Shkadov, G.M. Sisoev, Waves induced by instability in falling films of finite thickness, Fluid Dyn. Res. 35(5) (2004) 357–389.
[21] N.A. Malamataris, V. Balakotaiah, Flow structure underneath the large amplitude waves of a vertically falling film, AICHE J. 54 (2008) 1725–1740.
[22] H. Schlichting, Boundary-layer Theory, seventh ed., Mcraw-Hill, New York, NY, 1979.
[23] A. Solan, A. Zfati, Heat transfer in a laminar flow of a liquid film on a horizontal cylinder, Proceeding Fifth International Heat Transfer Conference, Tokyo, Japan, Paper FC 2.9 (1974) 90–93.